STEM CELLS AND DEVELOPMENT
Volume 22, Number 24, 2013

DOI: 10.1089/scd.2013.0313

In Vivo Implanted Bone Marrow-Derived Mesenchymal Stem Cells Trigger a Cascade of Cellular Events Leading to the Formation of an Ectopic Bone Regenerative Niche

Roberta Tasso,[1,2] Valentina Ulivi,[1,2] Daniele Reverberi,[2] Claudia Lo Sicco,[1,2] Fiorella Descalzi,[2] and Ranieri Cancedda[1,2]

We recently reported that mouse bone marrow stromal cells, also known as bone marrow (BM)-derived mesenchymal stem cells (MSCs), seeded onto a scaffold and implanted in vivo, led to an ectopic bone deposition by host cells. This MSCs capacity was critically dependent on their commitment level, being present only in MSCs cultured in presence of fibroblast growth factor-2. Taking advantage of a chimeric mouse model, in this study we show that seeded MSCs trigger a cascade of events resulting in the mobilization of macrophages, the induction of their functional switch from a proinflammatory to a proresolving phenotype, and the subsequent formation of a bone regenerative niche through the recruitment, within the first 2 weeks of implantation, of endothelial progenitors and of cells with an osteogenic potential (CD146+CD105+), both of them derived from the BM. Moreover, we demonstrated that, in an inflammatory environment, MSCs secrete a large amount of prostaglandin E_2 playing a key role in the macrophage phenotype switch.

Introduction

Bone marrow stromal cells (BMSCs), also known as BM-derived mesenchymal stem cells (MSCs), are considered effective therapeutic agents in a variety of clinical situations promoting the repair of injured tissues [1] not only for their multipotent differentiation potential, but also for their interesting role as cellular modulators [2–5]. However, it's still unknown why, in some cases, transplanted MSCs directly contribute to form a new tissue, whereas in others they activate endogenous mechanisms leading to new tissue formation by the host cells. This could be explained taking into account experimental evidences that indicate how different culture conditions promote the selection and the expansion of specific cell clones or subpopulations. It has been argued that the differentiation/senescence dynamics inherent to culture growth might work against stem cell retention or self-renewal [6]. Literature data indicate that the transplantation of cultures of human MSCs treated with fibroblast growth factor-2 (FGF-2) results in efficient bone formation, but abates the capacity of grafted cells to establish a hematopoietic microenvironment and to self-renew in vivo [7]. The bone formed within implants of human MSCs in immunodeficient mice during the early phases of ossification was shown to be of donor origin [8]. Chimerism has been described only at a later implantation stage, 8–12 weeks after surgery [9]. It must be noted that these and most of the similar literature studies, have been performed under xenogenic conditions, that is, implanting MSCs/scaffold combinations into recipients of other species. We previously reported that the murine MSCs capacity to activate endogenous regenerative mechanisms was critically dependent on their commitment level. We observed that MSCs expanded in vitro in the presence of FGF-2, but not MSCs expanded in the absence of the factor, were capable of inducing host regenerative responses in vivo leading to a bone formation by the recipient cells [10]. It therefore, appears that either the existence of species-specific intercellular signals, or the conditions of expansion in vitro, or both, could be critical in determining the nature and the origin of the cells playing a role in the new bone deposition.

To evaluate the cascade of cellular events activated by the implantation of scaffolds seeded with the FGF-2 expanded murine MSCs, we developed and implemented two models of ectopic bone formation. The first model involved the implantation of porous ceramic cubes seeded with mouse red fluorescent protein (RFP)-labeled MSCs into syngenic immunocopetent mice, with the aim of isolating and characterizing the inflammatory cells, such as macrophages, recruited within the pores of the scaffolds. In the second mouse model, lethally irradiated immunocompetent mice were hematopoietically reconstituted with green fluorescent

[1]Department of Experimental Medicine (DIMES), University of Genova, Genova, Italy.
[2]A.O.U. San Martino-IST, National Cancer Research Institute, Genova, Italy.

protein-positive (GFP^{pos}) syngeneic BM nucleated cells and used as hosts for transplants of combinations of bioceramic scaffolds and RFP-positive (RFP^{pos}) syngeneic MSCs. This chimeric mouse model allowed us to distinguish between donor implanted and recipient cells originated from the BM or from the surrounding tissues. Macrophage populations were initially mobilized as a consequence of the scaffold implantation, but the cascade of events that led to bone formation was started by MSCs secreting large amounts of prostaglandin E_2 (PGE_2). This prostaglandin was responsible of the functional switch of phenotype from proinflammatory (M1) to anti-inflammatory (M2) macrophages, which, in turn, led to the recruitment of endothelial progenitors ($CD133^{pos}$ $VEGFR2^{pos}$ $TLR2^{pos}$) and cells with an osteogenic potential ($CD146^{pos}CD105^{pos}$), both of them derived from the BM.

Materials and Methods

Mice

C57Bl/6 (MHC H2b haplotype) mice were purchased from Charles River Laboratories. GFP-transgenic mice [genotype C57BL/6-Tg (CAG-EGFP)1Osb/J] and RFP-transgenic mice [B6.Cg-Tg (CAG-DsRed*MST)1Nagy/J] were purchased from The Jackson Laboratory. Mice were used between 5 and 8 weeks of age. Mice were bred and maintained at the Institution's animal facility. The care and use of the animals were in compliance with the laws of the Italian Ministry of Health and the guidelines of the European Community.

BMSCs (MSCs) isolation and culture

Mice were euthanized, and BM cells were collected by flushing nucleated cells out of the femurs and tibiae with cold phosphate buffered saline (PBS), pH 7.2. Cells were cultured (15×10^6 nucleated cells/10 cm Petri dish) in Coon's modified F12 medium (Biochrom AG), supplemented with 10% fetal bovine serum (FBS; Lonza), 2 mM of L-glutamine, and 50 mg/mL of Penicillin/Streptomycin (standard medium). The cultures were performed in presence of 1 ng/mL of FGF-2 (Peprotech) (FGF + MSCs). Only cells from P1 or P2 passages were used for the implantation experiments. For in vitro experiments mimicking the inflammatory microenvironment, confluent MSCs were incubated for 24 h in standard medium containing 100 U/mL interleukin (IL)-1α. Cells were then extensively washed with PBS to remove residual stimulant factor and incubated in fresh medium with no supplements for an additional 24 h. Conditioned media were collected for western blot analysis or for macrophage treatment.

BM-derived macrophages isolation and culture

BM-derived macrophages were isolated from C57Bl/6 mice by flushing the BM with 5 mL of PBS. Obtained cells were washed in alpha-minimum essential medium (α-MEM) and plated in a 10 mm diameter cell culture dish for 2 h. The supernatant was replated in a nontreated cell culture dish and α-MEM supplemented with 10% FBS, 2 mM L-glutamine, 50 mg/mL Penicillin/Streptomycin and granulocyte macrophage-colony stimulating factor (GM-CSF) (25 μg/mL) was added (complete α-MEM). After 5 days, medium was removed and macrophages were divided in three groups: (1) macrophages cultured for 3 days in control medium (α-MEM), (2) macrophages cultured for 3 days in MSC-conditioned medium [serum free (SF)], (3) macrophages cultured for 3 days in IL-1α stimulated MSC-conditioned medium (IL-1).

$CD146^{pos}CD105^{pos}GFP^{pos}$ cells isolation and culture

$CD146^{pos}CD105^{pos}GFP^{pos}$ cells were isolated 11 days after implantation by cell sorting from MSC-seeded implants. Isolated cells were cultured in fibronectin-coated plates (BD Biosciences) and Coon's modified F12 medium supplemented with 10% FBS, 2 mM of L-glutamine, and 50 mg/mL of Penicillin/Streptomycin was added.

Surgical procedures

Bioceramic scaffolds were 100% synthetic calcium phosphate multiphase biomaterials containing 67% silicon-stabilized tricalcium phosphate (TCP) (Skelite™). These scaffolds had 60–65% porosity and were produced by Octane Medical Group (Kingston). All scaffolds were cubes with a dimension of about $4\times4\times4$ mm. After 3 or 4 weeks expansion, MSCs were detached from the dishes with 0.05% trypsin/ethylenediaminetetraaceticacid, washed in serum-free medium, and resuspended in aliquot at 2.5×10^6 cells per 20 μL fibrinogen (2.5 mg/mL) (Baxter). Each aliquot was seeded onto a scaffold to which 20 μL of murine thrombin (500 IU/mL) (Baxter) were then applied.

Recipient WT C57Bl/6 (nine mice/each considered time point; each mouse received four ectopic implants) or chimeric mice (12 mice/each considered time point; each mouse received four ectopic implants) were subcutaneously implanted with MSCs/bioscaffold constructs. Experiments were repeated at least three times. Some experiments included also groups of animals implanted with nonseeded, empty scaffolds. Groups of four animals were sacrificed after 3, 7, 11, and 15 days postimplantation, respectively, and the implants removed for further analysis.

Chimeric mouse model

Seventy-two C57Bl/6 recipient mice that have received a total body lethal radiation with 10 Gy were intravenously injected with 5×10^6 BM-nucleated cells derived from syngeneic GFP-Tg mice. Engraftment levels were assessed by the determination of the percentage of GFP^{pos} cells in the peripheral blood and BM of chimeric mice, 5 weeks post-transplantation.

Histological and immunohistochemical analysis

Formalin-fixed scaffolds were processed as previously reported [4]. Briefly, samples were decalcified with Osteodec (Bio-Optica) and embedded in paraffin using standard histological techniques. Four-micrometer serial sections were cut. Sections were stained with hematoxylin and eosin to reveal bone tissue. To detect the presence of $GFP^{pos}CD146^{pos}CD105^{pos}$ cells within the pores of the implants, 4-mm sections were treated with rabbit polyclonal anti-GFP antibody (clone A11122) (Molecular Probes Europe BV), followed by biotinylated goat anti-rabbit secondary antibody (Dako Cytomation). To detect the presence of RFP^{pos} MSCs within the pores of the implants, 4-mm sections were treated

with rabbit polyclonal anti-RFP antibody (Molecular Probes Europe BV), followed by the same biotinylated goat anti-rabbit secondary antibody. Negative controls with pre-immune serum and positive controls were run in parallel. Images were captured by transmitted light microscopy with an Olympus C3030 digital camera and Camedia Master Olympus software.

Cell sorting and flow-cytometric analysis

Cells, obtained by enzymatic digestions of RFP^{pos} MSC-seeded scaffolds from both wild-type (WT) and chimeric recipient mice, were washed twice and suspended in 500 μL PBS, and separated into RFP^{pos} and RFP^{neg} fractions at different times (1, 3, 7, 11, 15 days). Cells recovered after 11 days from implants conducted in chimeric mice underwent an additional sorting passage to separate GFP^{pos} $CD146^{pos}CD105^{pos}$ populations. All the experiments were performed using the cell sorter FACSAria (Becton Dickinson). $CD146^{pos}CD105^{pos}GFP^{pos}$ cells were cultured in the standard medium used for BMSC cultures. The immunophenotype of freshly-isolated RFP^{neg} cells obtained from both MSC-seeded and empty scaffolds and the immunophenotype of BM-derived macrophages cultured for 3 days in the presence of MSC-conditioned medium were analyzed by flow-cytometry using specific monoclonal antibodies. Antibodies for the flow-cytometric analysis were: monoclonal antibodies to CD11b (M1/70), CD31 (390), CD45 (30-F11), CD51 (RMV-7), CD86 (GL1), IA^b (AF6-120.1) (BD Pharmingen), monoclonal antibodies to CD36 (No.72-1), CD40 (1C10), CD133 (13A4), TLR2/CD282 (6C2) (eBioscience), monoclonal antibodies to Ly6C (1G7.G10), NK1.1 (PK136) (Miltenyi Biotec), monoclonal antibodies to CD105 (MJ7/18), CD206 (MR5D3), VEGFR2/CD309 (89B3A5) (BioLegend), monoclonal antibody to CD146 (P1H12) (Santa Cruz Biotechnology), and rabbit polyclonal to RAGE (Abcam).

All flow-cytometric analyses reported in this study were performed using the cell sorter FACSAria (Becton Dickinson). Data are expressed as percentages of positive cells and as ratio between mean fluorescence intensity (MFI) of cells stained with a specific antibody/MFI of correspondent isotype control (relative MFI).

Western blot analysis

Western blot analysis was performed as previously described [11]. Briefly, 5×10^5 cells were plated, the protein concentration of the lysate was measured using the Bradford method and equal protein amounts were used for western blot. Actin was blotted as an internal control. Equivalent amounts of corresponding conditioned media were analyzed. Sample were separated on NuPAGE™ 4–12% Bis-Tris gels (Invitrogen) and transferred to a Protran BA83 nitrocellulose membrane (Whatman GmbH). The blot was incubated with specific primary antibodies obtained from various sources.

Positive bands were revealed by an enhanced chemi-luminescence substrate mixture (GE Healthcare) and exposed to an X-ray film (GE Healthcare) to capture the image. Images were then scanned using the Epson perfection 1260 scanner, and band densities were quantified using the image J software (http://rsbweb.nih.gov/ij/download.html). Mean pixel densities were transferred to excel file formats and means and standard deviations (SDs) were obtained for statistical analysis. Antibodies against CXCL1/KC and Lipocalin-2 (Lcn-2) were purchased from R&D Systems. Antibodies to cycloxygenase 2 (COX-2), mPGES-1, $hPGD_2$ synthase were from Cayman Chemical; anti-actin antibody was supplied by Santa Cruz Biotechnology.

PGE_2 and $15\Delta PGJ_2$ quantitation

Confluent MSCs were incubated in serum-free basal medium supplemented or not supplemented with 100 U/mL IL-1α for 24 h. Cells were then extensively washed with PBS to remove residual stimulant factor and incubated in serum-free medium for an additional 24 h after which media were collected, centrifuged to remove particulate matter and stored at −80°C. Aliquots were assayed for PGE_2 content using a PGE_2-specific competitive EIA kit-Monoclonal (Cayman Chemical) according to the manufacturer's instructions. A $15\Delta PGJ_2$ specific competitive EIA kit (Enzo Life Sciences, Inc.) was used according to the manufacturer's instructions. Each sample was measured in triplicate in two dilutions. Statistical analysis of the data was performed.

Nuclear factor-kappa B activation

Binding of the nuclear factor-kappa B (NF-kB) p65 subunit to the NF-kB binding consensus sequence 5′-GGGACTTTCC-3′ was measured with the enzyme linked immunosorbent assay-based Trans Am NF-kB kit (Active Motif) using whole cell lysates prepared from MSC cultures, as recommended by manufacturer. All measurements were performed in triplicate. The Trans-Am kit employs 96-well microtiter plates coated with an oligonucleotide containing the NF-kB binding consensus sequence. The active form of p65 subunit in the whole cell lysates was detected using antibodies specific for an epitope that is accessible only when the subunit is activated and bound to its target DNA. Specificity was checked by measuring the ability of soluble WT or mutated oligonucleotides to inhibit binding. Results are expressed as specific binding, that is, the absorbance values observed in the presence of the mutated oligonucleotide minus those observed in the presence of the WT oligonucleotide.

Statistical analysis

In this study, results are given as the mean values ± SD. All statistical analyses were performed using GraphPad software. The two-tailed Student's *t*-test was performed. A value of $P<0.05$ was considered significant.

Results

Different macrophage populations infiltrate the implanted scaffolds

We previously reported the enhancement of some biological processes, including inflammation and innate immunity in MSCs grown in FGF-2 [10]. In particular, chemokines implicated in monocyte recruitment from the blood to inflamed tissues, such as CCL8 (monocyte chemoattractant protein 2) and CCL9 (macrophage inflammatory protein-1 gamma), were oversecreted. Monocytes/macrophages (MC/Mph) led the inflammatory cascade reaction guiding revascularization and tissue repair/regeneration at injury sites [12–14]. To investigate whether implanted MSCs could trigger the mobilization of macrophages and could alter the balance between M1

(CD86+/CD40+) and M2 (CD206+/CD51+) phenotypes, we analyzed the nature of the host macrophages recruited within the pores of both RFP^{pos} MSC-seeded and control empty scaffolds after implantation in vivo in C57Bl/6 immunocompetent WT mice. Implants were harvested at different times, and collagenase-digested to generate single cell suspensions. Recovered cells were sorted, based on RFP expression, to separate implanted RFP^{pos} MSCs and recruited RFP^{neg} cells.

The flow-cytometric analysis of host derived RFP^{neg} cells extracted from the scaffolds at 1, 3, and 7 days after implantation showed that macrophages infiltrated both types of ectopic implants, although the balance between M1 (CD86+/CD40+) and M2 (CD206+/CD51+) populations was directly correlated to the presence of the seeded MSCs.

The analysis of the immunophenotype of the host cells recovered from control empty scaffolds 1 and 3 days after implantation evidenced an increased relative MFI of the typical M1 markers compared to host cells extracted at the same times from the MSC-seeded scaffolds (Supplementary Fig. S1A, B; Supplementary Data are available online at www.liebertpub.com/scd and Table 1). Indeed, the expression of the two main M1 markers, CD40 and CD86, turn out to be significantly higher in the cells extracted from the empty scaffolds. On the contrary, recruited cells extracted from MSC-seeded scaffolds after 1 and 3 days showed an increased expression of the markers typically associated with a M2 phenotype. In particular, the relative MFI associated with CD51, CD206, and receptor for advanced glycation end products (RAGE) were significantly increased in cell-seeded implants. In particular, RAGE is known to be involved in tissue damage and chronic inflammatory disorders, and to sustain the inflammatory response upon engagement with damage associated molecular pattern molecules (DAMPs), such as high mobility group box 1 (HMGB1) [15]. At the last considered time (day 7 after implantation), we observed a general reduction in the expression of all macrophage-specific markers, although the cell surface antigen CD86, associated with the M1 phenotype, remained significantly more expressed by host cells extracted from empty scaffolds, whereas the cell surface antigens CD206 and CD51, associated with the M2 profile, were still significantly more expressed by cells recovered from MSC-seeded scaffolds (Supplementary Fig. S1C; Table 1). To confirm whether the heterotopic implantation of MSCs could induce a strong inflammatory reaction, we performed also a histological analysis on sections obtained from the previously described implants (RFP^{pos} MSC/scaffold constructs implanted in syngeneic immunocompetent WT mice). After 3 days of implantation, a strong inflammatory infiltrate was present within the pores of the scaffolds (Supplementary Fig. S2A), confirming the flow-cytometric analysis conducted at the same time point (Supplementary Fig. S1B).

The inflammatory milieu decreased after 7 days of implantation, when a predominant fibrous connective tissue was observed (Supplementary Fig. S2B) in agreement with the decrease in the percentages of macrophage populations analyzed at this time point (Supplementary Fig. S1C).

Table 1. Relative Mean Fluorescence Intensity of Macrophage Markers on Host-Derived Cells Recruited at Different Times Within MSC-Seeded and Control Empty Scaffolds

	Relative MFI empty scaffold (average ± SD)	*Relative MFI MSC-seeded scaffold (average ± SD)*	*Statistical significance (two-tailed P value)*
Cells recovered 1 day after implantation			
CD11b	4.52 ± 0.94	2.85 ± 0.42	Not statistically significant
CD40	6.31 ± 1.10	1.00 ± 0.07	0.0011
CD86	14.90 ± 3.81	0.86 ± 0.09	0.0031
CD36	1.62 ± 0.07	4.37 ± 1.80	Not statistically significant
CD206	3.37 ± 1.12	11.30 ± 2.98	0.0125
CD51	2.53 ± 0.84	7.75 ± 1.96	0.0133
RAGE	1.30 ± 0.37	1.78 ± 0.46	Not statistically significant
Cells recovered 3 days after implantation			
CD11b	10.10 ± 3.76	2.58 ± 0.97	0.0285
CD40	12.35 ± 3.89	1.44 ± 0.02	0.0083
CD86	9.19 ± 2.12	2.32 ± 0.47	0.0054
CD36	1.68 ± 0.90	9.40 ± 2.52	0.0075
CD206	1.00 ± 0.08	18.40 ± 4.76	0.0032
CD51	1.50 ± 0.05	8.39 ± 2.78	0.0127
RAGE	1.19 ± 0.08	10.05 ± 3.47	0.0115
Cells recovered 7 days after implantation			
CD11b	3.33 ± 1.86	4.74 ± 1.34	Not statistically significant
CD40	4.07 ± 1.99	1.26 ± 0.08	Not statistically significant
CD86	3.04 ± 0.96	1.24 ± 0.06	0.0316
CD36	1.05 ± 0.04	3.04 ± 1.77	Not statistically significant
CD206	1.15 ± 0.10	14.07 ± 4.98	0.0109
CD51	1.05 ± 0.06	5.85 ± 2.12	0.0172
RAGE	2.85 ± 0.36	7.02 ± 3.01	Not statistically significant

MFI, mean fluorescence intensity; SD, standard deviation; MSC, mesenchymal stem cell.

After 11 days, the fibrous tissue was the main component within the pores of the scaffolds (Supplementary Fig. S2C).

To better define the balance between macrophages with M1 and M2 phenotypes at different implantation times, we performed two consecutive sorting passages. Implants, harvested at different times, were collagenase-digested to generate single cell suspensions. The first sorting passage, based on RFP expression, was performed to separate donor RFP^{pos} MSCs from recipient RFP^{neg} recruited cells. The second sorting passage was carried out to isolate, from the bulk of RFP^{neg} recruited cells, macrophages with proinflammatory (M1) and anti-inflammatory (M2) characteristics. CD86 and CD40 were selected as M1 markers, CD206 and CD51 as M2 markers. M1 ($CD86^{pos}CD40^{pos}$) and M2 ($CD206^{pos}CD51^{pos}$) macrophages were isolated from the host cells recovered from empty scaffolds and from the RFP^{neg} populations extracted from MSC-seeded scaffolds (Supplementary Fig. S3). We detected a higher percentage of M1 cells infiltrating the empty scaffolds compared to the MSC-seeded ones. This difference was statistically significant 1 and 7 days after implantation in vivo (Fig. 1A). Conversely, implanted MSCs induced a significantly augmented infiltration of M2 cells at day 3 and 7 (Fig. 1B). Moreover, the ratio between M2 and M1 cells (M2/M1) progressively increased from day 1 to 7 in the populations recovered from the scaffolds seeded with MSCs, whereas it remained constant in the populations isolated from the nonseeded implants (Fig. 1C).

Quantification of cytokine expression by real-time polymerase chain reaction in M1 and M2 cells isolated from both types of implants confirmed the nature of the two recovered cell populations. Being the differences relative to the expression of M1 and M2 markers more pronounced 3 days after in vivo implantation, we performed this analysis on the cells sorted at day 3. Compared to the M2 counterparts, M1 cells isolated from both types of implants had higher expression of both the proinflammatory cytokine tumor necrosis factor-α (TNF-α) (M1 Empty scaffold vs. M2 Empty scaffold: $P<0.005$; M1 MSC-seeded scaffold vs. M2 MSC-seeded scaffold: $P<0.025$) and HMGB1 (M1 Empty scaffold vs. M2 Empty scaffold: $P<0.0001$; M1 MSC-seeded scaffold vs. M2 MSC-seeded scaffold: $P<0.0001$) (Supplementary Fig. S4A, B). HMGB1 is a nuclear protein that can act as a cytokine to regulate different biological processes, such as inflammation, cell migration and metastasis. HMGB1 directs the migration of vascular and transformed cells. It has been described that RAGE, as well as the members of the toll-like receptors TLR-2 and TLR-4, binds HMGB1, causing the activation of different cell pathways, such as NF-kB, ERK1/2, and p38.

A higher expression of IL-10, an anti-inflammatory cytokine, was instead detected in the M2 populations isolated from both empty and MSC-seeded scaffolds (M1 Empty scaffold vs. M2 Empty scaffold: $P<0.05$; M1 MSC-seeded scaffold vs. M2 MSC-seeded scaffold: $P<0.001$) (Supplementary Fig. S4C).

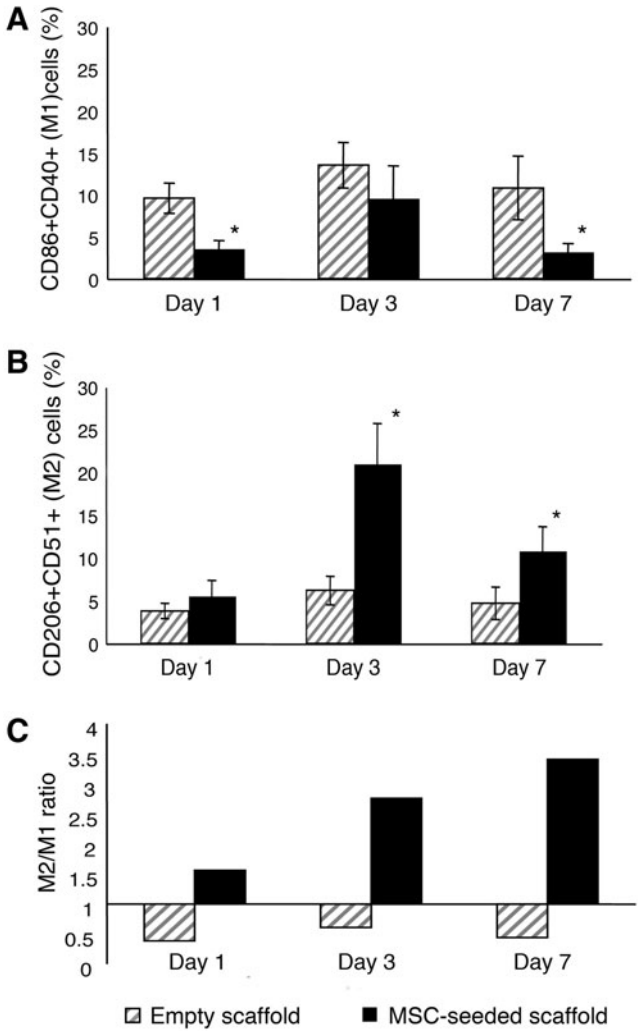

FIG. 1. Quantification of M1 and M2 macrophages recovered from empty and bone marrow stromal cell (BMSC)-seeded scaffolds. Percentage of M1 (CD86 + CD40+) **(A)** and M2 (CD206 + CD51+) **(B)** macrophages isolated 1, 3, and 7 days after implantation of both control empty and mesenchymal stem cell (MSC)-seeded scaffolds. In **(A)**, "*" indicates $P<0.05$, comparing the percentage of CD86 + CD40+ M1 cells isolated from control empty scaffolds to the percentage of M1 cells isolated from MSC-seeded scaffolds after 1 and 7 days. In **(B)**, "*" indicates $P<0.05$, comparing the percentage of CD206 + CD51+ M2 cells isolated from MSC-seeded scaffolds to the percentage of M2 cells isolated from control empty scaffolds. **(C)** Ratio between M2 (CD206 + CD51+) and M1 (CD86 + CD40+) macrophages isolated from empty and MSC-seeded scaffolds at different implantation times. All results are averaged from three independent experiments, and data are represented as mean ± standard deviation (SD).

MSC-secreted PGE_2 promotes the switch of proinflammatory macrophages to an alternatively activated phenotype

MSCs are very sensitive to inflammatory stimuli [16,17]. Since the injury generated by the ectopic implant induces per se a strong inflammatory response, we mimicked in vitro the inflammatory environment surrounding the implanted MSCs to investigate whether the activated microenvironment affected the release of factors possibly involved in the macrophage functional switch. MSC confluent monolayers, were treated either with SF medium or SF medium supplemented with 100 U/ml IL-1α (IL-1). After 24 h, culture media

were replaced with fresh medium with no supplements and cells were incubated for additional 24 h before media collection. To evaluate the direct effect of MSC-released factors on the macrophage phenotype, collected conditioned media were used to treat cultures of BM-derived MC/Mph. The flow-cytometric analysis of the MC/Mph isolated before and after the treatments showed that, when the cells were cultured in standard α-MEM (no conditioned medium treatment), they expressed high levels of the proinflammatory immature markers CD11b and Ly6C (48.2% + 9.7 and 61.6% + 18.5, respectively; Supplementary Fig. S5, upper panels). In these culture conditions, the expression of protein markers of classically activated M1 macrophages, such as CD40 and CD86, was less than 2% (Supplementary Fig. S5, middle panels). Moreover, the BM-MC/Mph did not express any of the typical M2 markers, such as the scavenger receptor CD36, the mannose receptor CD206, or the $\alpha_v\beta_3$ integrin CD51 (Supplementary Fig. S5, lower panels). The frequency of Ly6C + macrophages decreased after 3 days of treatment with MSC-conditioned medium (SF) compared to treatment with the control standard medium (α-MEM), although this difference was not statistically significant. The percentage of Ly6C + cells decreased significantly when MC/Mph were cultured with the conditioned medium obtained from IL-1-stimulated MSCs ($P < 0.05$; Fig. 2). Interestingly, the percentage of CD206-expressing macrophages significantly increased after the cell treatment with both SF and IL-1 conditioned media ($P < 0.025$ and $P < 0.025$; Fig. 2).

A characterization of the pathways activated in MSCs cultured in inflammatory conditions was performed and we searched for bioactive molecules released in the culture media capable of turning the macrophage phenotype into a proresolving profile.

We observed that the IL-1 treatment strongly increased NF-kB activity in the MSCs compared to the no supplement control ($P < 0.0001$; Fig. 3A). In parallel, we checked the synthesis and secretion of keratinocyte chemoattractant (KC) and Lcn-2. The amount of both KC and Lcn-2 present in the conditioned media of IL-1-stimulated MSCs was significantly increased ($P < 0.002$ and $P < 0.0001$; Fig. 3B, C). Moreover, IL-1 treatment induced in the MSCs the expression of COX-2 and the downstream enzyme mPGE synthase, whose products play a key role in the inflammatory cascade leading to the acute phase response [11]. It is noteworthy that PGD synthase expression level was unaffected (Fig. 3D).

In agreement with these findings, PGE_2 production and secretion in MSC-culture medium was strongly induced by the IL-1 treatment, increasing from 3.7 + 1.1 ng/mL in SF medium up to 29.5 + 11 ng/mL in the medium of cells maintained in inflammatory conditions ($P < 0.0001$; Fig. 3E). The production and secretion of the PGD_2 metabolite 15 ΔPGJ2 was only slightly reduced (Fig. 3E). PGE_2 has been described to modulate the cytokine profile of macrophages [18,19]. To establish a possible involvement of MSC-secreted PGE_2 in the macrophage functional switch from a proinflammatory to an anti-inflammatory phenotype, BM-derived MC/Mph were stimulated with conditioned media from: (1) MSCs cultured in SF medium without any further supplement (SF); (2) supplemented with IL-1α (IL-1); (3) supplemented with the COX-2 specific inhibitor NS-398 to block PGE_2 production (NS-398); (4) supplemented with IL-1α and NS-398 (IL-1 + NS-398). MSC-conditioned media from cells incubated in the presence of the inhibitor NS-398 yielded less than 1% of $CD206^{pos}$ macrophages; thus, indicating that a COX-2 product was involved in the macrophage switch (Fig. 4). The involvement of PGE_2 in the BMSC-induced macrophage polarization was confirmed by the observation that the percentage of recovered $CD206^{pos}$ cells progressively augmented when macrophages were cultured in (IL-1 + NS-398)-MSC conditioned medium supplemented with increasing concentrations of PGE_2. The PGE_2 concentrations tested ranged from 1 to 100 nM, being the intermediate concentration (15 nM) roughly equivalent to the concentration of PGE_2 found in the SF condition, and the highest dose (100 nM) equivalent to the concentration found in the medium of IL-1-treated MSCs (Fig. 3E, left panel). Less than 3% of $CD206^{pos}$ cells were detected when PGE_2 was added at the lower concentration (1 nM) (Fig. 4), whereas a statistically significant increase in the percentage of $CD206^{pos}$ cells was observed when PGE_2 was used at 15 and 100 nM ($P < 0.02$ and $P < 0.005$) (Fig. 4).

Taken together, these data demonstrate that MSCs responded to the inflammatory environment activating NF-kB and secreting PGE_2, in turn, triggering the functional switch of macrophages from the inflammatory M1 to the anti-inflammatory M2 phenotype.

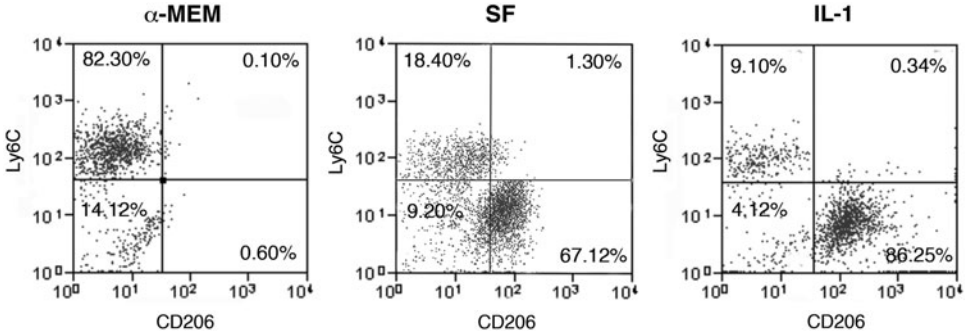

FIG. 2. Phenotypic characterization of cultured BM-derived macrophages treated with MSC-conditioned medium. Flow-cytometric analysis of BM-macrophages cultured for 3 days in control standard medium alpha-minimum essential medium (α-MEM), in MSC-conditioned medium [serum free (SF)], and in conditioned medium derived from interleukin (IL)-1α stimulated MSCs (IL-1). CD206 was selected as marker of anti-inflammatory macrophages, Ly6C as marker of proinflammatory macrophages. Results show one representative experiment, and five independent experiments were performed.

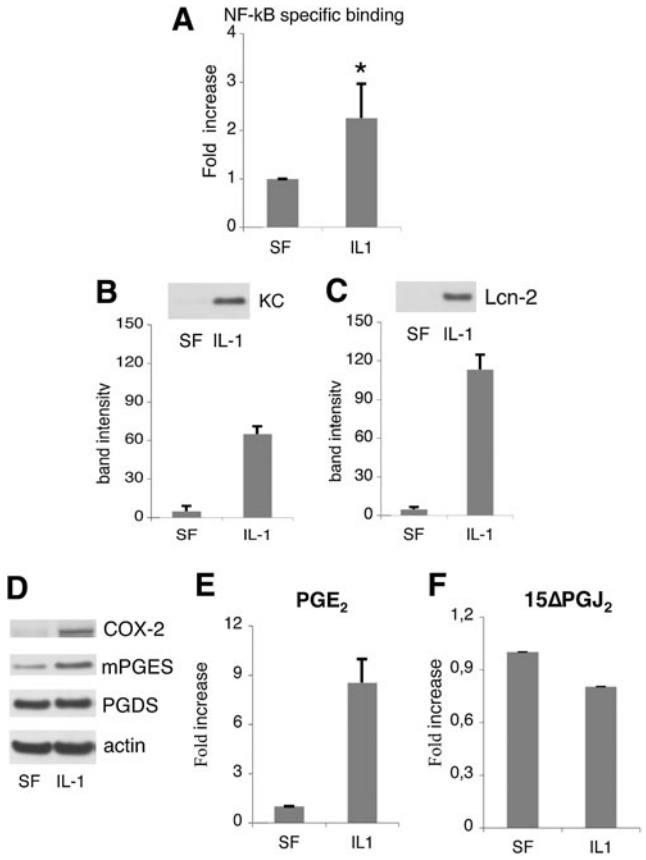

FIG. 3. Activation of nuclear factor-kappa B (NF-kB)-dependent inflammatory pathways in MSCs in response to IL-1α. **(A)** Ten milligrams of cell lysate was tested for binding of the activated p65 NF-kB subunit to an NF-kB consensus sequence. Results are expressed as specific binding. The averages of three experiments each one performed in triplicate are shown as average ± standard error of the mean (SEM); $^*P < 0.0001$, comparing the activity of NF-kB in MSCs and in no supplement control. **(B, C)** Modulation of KC and Lcn-2 secretion. After incubation with the factors cells were washed with PBS, and incubated with SF medium for 24 h before conditioned medium collection. *Left panels*: western blot of MSC-conditioned media with specific antibodies. *Right panels:* Average densitometric analysis ± SD of five western blots performed on five independent experiments. **(D)** Western blot of MSC lysates with specific antibodies. **(E)** prostaglandin E_2 (PGE_2) and **(F)** $15\Delta PGJ_2$ content in MSC-conditioned media. All values were normalized to the value of the unstimulated sample. The averages of three experiments each one performed in triplicate are shown as average ± SEM.

Mobilization of BM-derived endothelial progenitor cells into MSC-seeded scaffolds

We previously reported that the neovascularization of the implants was one of the first host responses to the graft and that cells with endothelial features could be recovered from the scaffolds 7 days after implantation in vivo [5]. By flow-cytometric analysis, we checked for the presence of endothelial progenitor cells (EPCs) in the host cell population migrated into scaffolds either seeded or not seeded with BMSCs after 7 days of implantation. Implants were performed in chimeric mice lethally irradiated and reconstituted with GFP^{pos} donor BM cells to identify the possible BM origin of the mobilized cells. We harvested the implants, recovered the cells through an enzymatic digestion, and sorted out the RFP^{pos} cells originally seeded on the scaffold (Fig. 5A). We observed the presence of GFP^{pos} BM-derived cells within the RFP^{neg} recruited host cells from both empty scaffold and MSC-seeded scaffold (gate R6), although to a different extent [27.5% + 6.8 and 49.8 + 12.6, respectively; Fig. 5B (upper panel), C (upper panel)]. Since EPCs express the HMGB1 receptor TLR2 [20], we searched for TLR2-expressing cells within the recruited populations. All the $TLR2^{pos}$ cells were BM derived, being also GFP^{pos} [Fig. 5B (bottom-left panel), C (bottom-left panel)]. Among the $TLR2^{pos}GFP^{pos}$ populations (gate R11), observed in both types of implants, we searched for cells coexpressing CD133 and VEGFR2, whih are specific markers of EPCs. A 4.3% of $CD133^{pos}VEGFR2^{pos}$ EPCs was detected within the cells from MSC-seeded scaffold (gate R16) (Fig. 5C, bottom-right panel). No EPCs were observed in the cells from the control empty scaffold (Fig. 5B, bottom-right panel); thus, indicating that the paracrine activity mediated by implanted MSCs was crucial in triggering the specific recruitment of BM-derived EPCs, the main responsible for vasculogenesis.

To evaluate whether the recruited EPCs could differentiate into mature endothelial cells (ECs), we checked for the presence of CD31-expressing cells in the bulk of the host-derived population after 15 days from implantation in vitro. $CD31^{pos}GFP^{neg}$ ECs were recovered from both implanted empty scaffolds and MSC-seeded scaffolds, indicating that a sprouting phenomenon from surrounding pre-existing vessels occurred in both types of implants (Fig. 5D). On the contrary, $CD31^{pos}GFP^{pos}$ ECs were present only in the MSC-seeded scaffolds, confirming the presence of BM-derived mature ECs possibly differentiated from the previously described recruited EPCs (Fig. 5D).

BM-derived $CD146^{pos}CD105^{pos}$ cells are recruited into the bone regenerative niche

We previously reported that $CD146^{pos}$ host cells with an osteogenic potential were mobilized into the MSC-seeded scaffolds and that the bone observed within the pore of the scaffold after 60 day implantation was derived from host cells [5] (see also Supplementary Fig. S6). Microvascular and BM pericytes are characterized by the expression of the cell surface marker CD146 [7,21], and in addition to play an important role in the stabilization of nascent capillaries and prevention of vascular regression [22], they possess mesenchymal plasticity and robust mesodermal developmental potential [21]. However, CD146 antigen is expressed by a variety of mouse cells, including myeloid, ECs, and natural killer T cells (NKT). To investigate whether tissue resident/local pericytes or BM-derived pericyte-like cells migrated toward the bone regenerative niche, scaffolds, either seeded or not seeded with MSCs, were implanted in the chimeric mouse model, harvested after 11 days, and enzymatically digested to recover migrated cells (Fig. 5A). To evaluate the authentic contribution of $CD146^{pos}$ cells in the regenerative process, we checked the sorted RFP^{neg} host cells for the presence of cells coexpressing CD146 with: (1) the mesenchymal marker CD105; (2) the myeloid marker CD45; (3) the typical NKT cells marker NK1.1. The flow-cytometric analysis

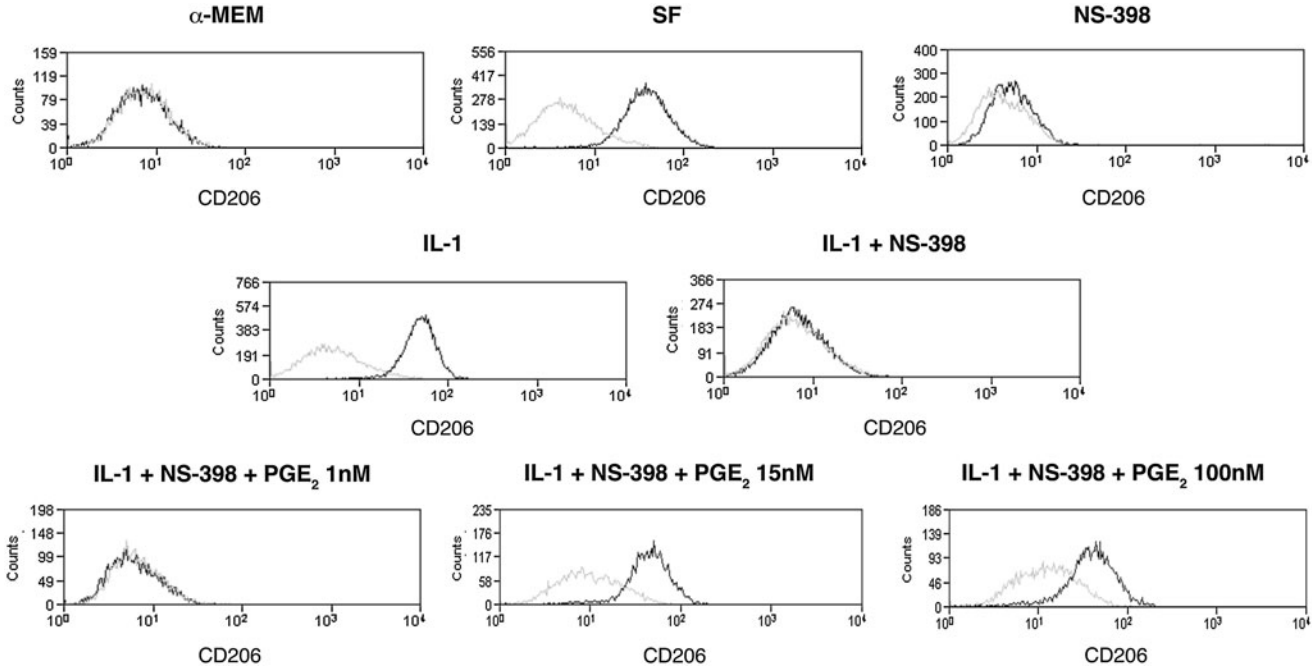

FIG. 4. Effect of the PGE_2 content in MSC-conditioned culture media on macrophage switch from M1 to M2 profile. Flow-cytometric analysis of BM-macrophages cultured for 3 days in: control standard medium (α-MEM); MSC-conditioned medium (SF); MSC-conditioned medium supplemented with the COX-2 specific inhibitor NS-398 (NS-398); conditioned medium derived from IL-1α stimulated MSCs (IL-1); conditioned medium derived from IL-1α stimulated MSCs and supplemented with NS-398 (IL-1 + NS-398); and (IL-1 + NS-398) conditioned medium supplemented with different concentrations of PGE_2 (1, 15, and 100 nM) (IL-1 + NS-398 + PGE_2 1 nM, IL-1 + NS-398 + PGE_2 15 nM, IL-1 + NS-398 + PGE_2 100 nM, respectively). CD206 was selected as marker of M2 macrophages. The *black line* represents the expression of the specific marker on tested cell populations. The *gray line* indicates nonreactive immunoglobulin of the same isotype, which was included as a negative control. Presented data refer to one representative experiment.

of the host-derived cell population isolated from control empty scaffolds revealed that 17.6% of the cells migrated into the ectopic implants were BM-derived GFP^{pos} cells (Fig. 6A, upper-left panel). Nevertheless no $CD146^{pos}CD105^{pos}$ cells were present, while 13.9% of $CD146^{pos}$ cells expressed the nonspecific marker CD45 and the 3.1% coexpressed the marker NK1.1 (Fig. 6A, upper-right, bottom-left, and bottom-right panels, respectively).

Isolated host-derived RFP^{neg} cells obtained from MSC-seeded scaffolds underwent an additional sorting passage to separate BM-derived GFP^{pos} from GFP^{neg} cells. Both RFP^{neg} GFP^{pos} and RFP^{neg} GFP^{neg} populations were cytofluorimetrically analyzed to confirm the successful outcome of the sorting steps. Since some GFP^{neg} contaminating cells were present in the initially sorted RFP^{neg} GFP^{pos} population, only confirmed GFP^{pos} cells (Gate R6 in Fig. 6B, upper-left panel) were considered for further analysis. Instead, no contaminant GFP^{pos} cells were present in the sorted RFP^{neg} GFP^{neg} population (Fig. 6C, upper-left panel).

Only the GFP^{pos} population was characterized for the presence of a large number of cells coexpressing the myeloid marker CD45 and the CD146, whereas the GFP^{neg} population was characterized by [Fig. 6B (bottom-left panel), C (bottom-left panel)]. In both populations, less than 1% of $CD146^{pos}$ cells coexpressed the NKT marker NK1.1 [Fig. 6B (bottom-right panel), C (bottom-right panel)]. Interestingly, the 5.6% of BM-derived GFP^{pos} cells coexpressed the mesenchymal markers CD146 and CD105 (Fig. 6B, upper-right panel), whereas no $CD146^{pos}CD105^{pos}$ cells were observed in the GFP^{neg} counterpart (Fig. 6C, upper-right panel).

$CD146^{pos}CD105^{pos}GFP^{pos}$ cells were isolated by cell sorting from the MSC-seeded scaffold and culture-expanded utilizing the same medium used for MSC cultures (Fig. 7A). After 2 months of culture, cells still expressing high levels of GFP, CD105, and CD146 (Fig. 7B) were tested for their osteogenic differentiation potential in vivo. Cell seeded scaffolds were subcutaneously implanted into immunocompetent syngeneic recipient mice. The histological analysis of transplants harvested after 60 days revealed the presence of a forming bone within the pores of the scaffolds (Fig. 7C). Immunohistochemical analysis revealed that the cells entrapped in the bone matrix were GFP^{pos}; thus, indicating that the bone tissue was of donor origin (Fig. 7C).

Discussion

Although the improvement observed in injured tissues after administration of exogenous stem/progenitor cells could be due to their direct engraftment and differentiation to replace injured cells, it became evident that in many situations the exogenous progenitors acted by producing bioactive factors without a significant engraftment and differentiation [2,23,24]. We recently reported that in an ectopic bone formation model, BM-derived stromal cells implanted in vivo triggered regenerative mechanisms by recruiting specific host cells in the bone regenerative niche

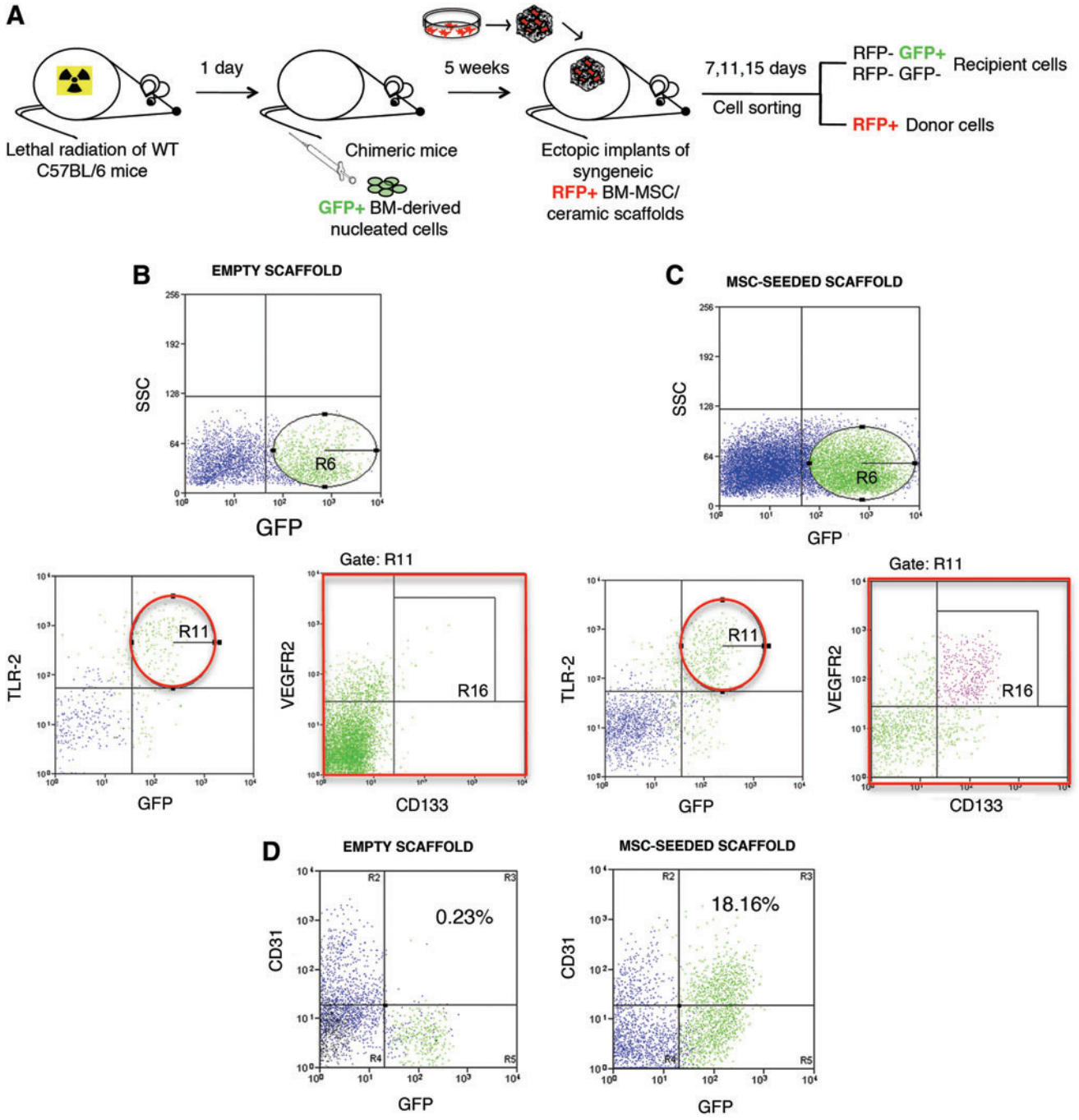

FIG. 5. Phenotypic characterization of host-derived endothelial cells recovered from scaffolds implanted for 7 days in chimeric mice. **(A)** Representative cartoon of experimental procedures of the ectopic bone formation model performed in chimeric mice. **(B)** Representative flow-cytometric analysis of cells recovered from empty scaffolds. **(C)** Representative flow-cytometric analysis of cells recovered from MSC-seeded scaffolds. In both **(B, C)** the *upper panels* show the green fluorescent protein-positive (GFP^{pos}) BM-derived cells (gate R6). The *bottom-left panels* show the coexpression of TLR2 and GFP (gate R11). The *bottom-right panels* show the coexpression of CD133 and VEGFR2 among the $TLR2^{pos}GFP^{pos}$ population. Gate R16 indicates the BM-derived $CD133^{pos}VEGFR2^{pos}TLR2^{pos}GFP^{pos}$ population. **(D)** *Left* and *right panels* show the coexpression of CD31 and GFP in cells recovered 15 days after implantation from control empty and MSC-seeded scaffolds, respectively. Color images available online at www.liebertpub.com/scd

[4,5,25]. Since we used BM cell cultures of passage 1 or 2 for the implantation experiments, to rule out the possibility that a massive presence of contaminating macrophages could have played an important role in eliciting the effects attributed exclusively to MSCs, we performed experiments in which we implanted scaffolds loaded with $CD45^{neg}$ MSCs further depleted of the CD11b+ and CD14+ components. Also in that case, we observed a new bone tissue of host origin formed within the implants 60 days after implantation [4].

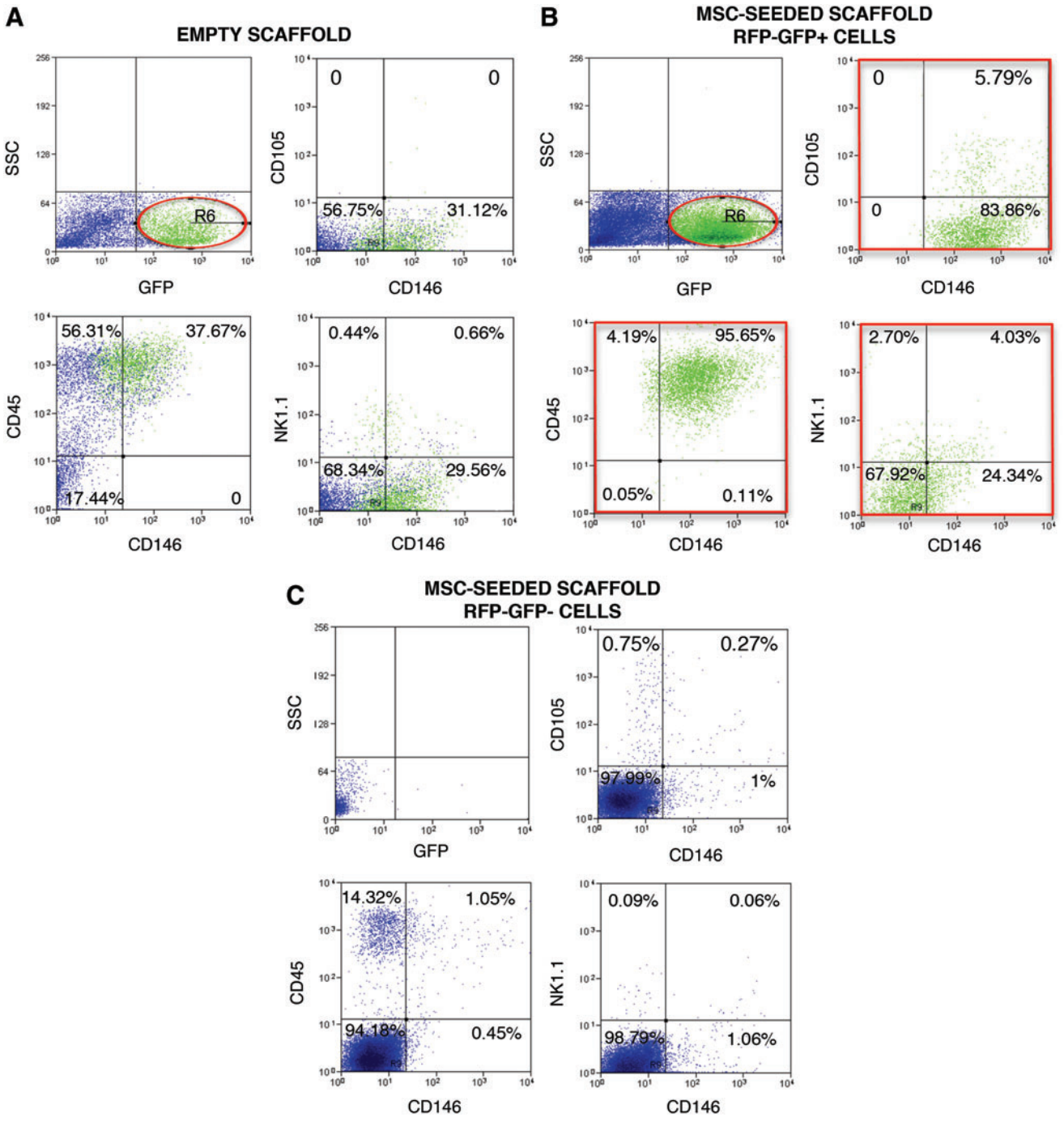

FIG. 6. Phenotypic characterization of host derived CD146+ recovered from scaffolds implanted for 11 days in chimeric mice. **(A)** Representative flow-cytometric analysis of cells recovered from empty scaffolds. **(B)** Representative flow-cytometric analysis of cells recovered from MSC-seeded scaffolds and sorted to isolate the host (RFP^{neg}) BM-derived (GFP^{pos}) recruited cell population. **(C)** Representative flow-cytometric analysis of cells recovered from BMSC-seeded scaffolds and sorted to isolate the host (RFP^{neg}) locally resident (GFP^{pos}) recruited cell population. In **(A–C)** the *upper-left panels* show the GFP^{pos} BM-derived cells (gate R6). The *upper-right panels* show the percentage of CD146+ cells coexpressing the mesenchymal marker CD105; the *bottom panels* show the coexpression of CD146 and the myeloid marker CD45 (*left panel*) and the NKT marker NK1.1 (*right panel*). Color images available online at www.liebertpub.com/scd

In this study, we show that implanted MSCs generated a cascade of events resulting in the mobilization of cells of the innate immune system, such as macrophages, the induction of their functional switch from a proinflammatory to a proresolving phenotype, and the recruitment of BM-derived specific progenitors with vasculogenic and osteogenic properties. Moreover, we demonstrated that MSCs, in an inflammatory environment, secreted a large amount of PGE_2 playing a key role in the macrophage polarization.

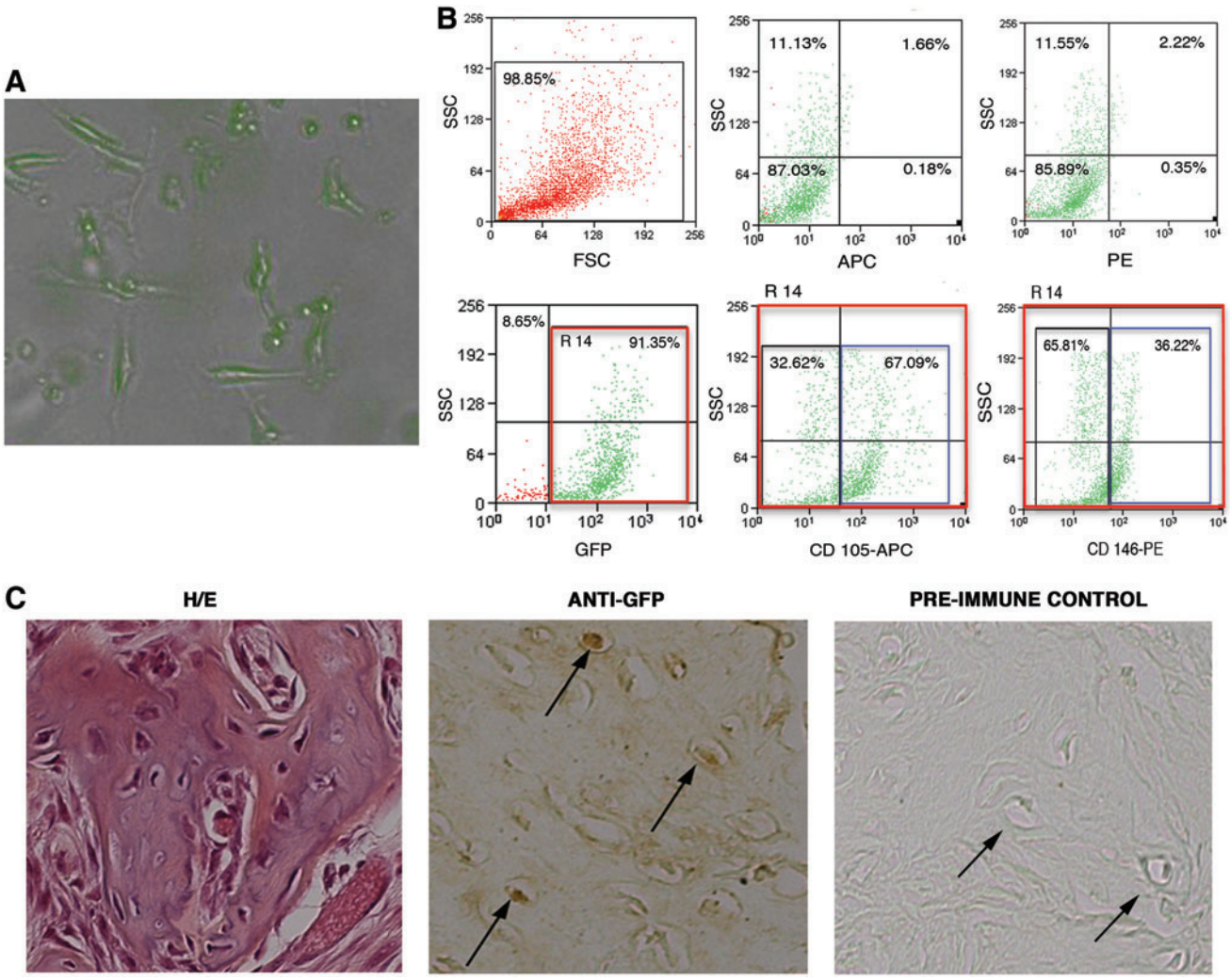

FIG. 7. In vitro and in vivo analysis of cultured CD146^{pos}CD105^{pos}GFP^{pos} cells isolated from MSC-seeded scaffolds 11 days after implantation in vivo. **(A)** Morphological analysis of cultured cells expressing the GFP. Cells were observed with the Apotome Microscope Technique from Carl Zeiss. **(B)** Flow-cytometric analysis of cultured CD146^{pos}CD105^{pos}GFP^{pos} cells. *Upper-left panel*: representative dot-plot of the physical properties; *bottom-left panel*: endogenous GFP expression (gate R14); *bottom-middle* and *bottom-right panels* represent the percentage of GFP^{pos} cells (R14) coexpressing CD105 (APC) and CD146 (PE), respectively; *upper-middle* and *upper-right panels* represent the same nonlabeled cells, plotted using fluorescence parameters (negative controls). **(C)** In vivo osteogenic differentiation of cultured CD146^{pos}CD105^{pos}GFP^{pos} cells. *Left panel*: representative Hematoxylin/eosin (H/E) staining of CD146^{pos}CD105^{pos}GFP^{pos}-seeded scaffolds after 60 days of implantation in vivo; *middle panel*: representative immunohistochemical analysis performed using a specific anti-GFP Ab on sections derived from CD146^{pos}CD105^{pos}GFP^{pos}-seeded scaffolds; *right panel* represents the preimmune control of the anti-GFP staining. *Arrows* indicate GFP+ osteoblasts. Color images available online at www.liebertpub.com/scd

Among the several biological functions hypothesized as related to the trophic effects of MSCs [26], the most significantly upregulated by FGF-2 were immune response, inflammatory response, response to wounding, and chemotaxis; thus, suggesting that a "wound" signature was induced in MSCs in presence of this factor [10]. Indeed, the bulk of cytokines and chemokines upregulated in treated cells contributed to orchestrate a microenvironment typically activated during wound healing and repair. We tested the hypothesis that the appearance of a localized host-derived bone tissue in grafts conducted with MSCs cultured in presence of FGF-2 could be mediated by cellular events also occurring in wound healing, and involving the recruitment of competent cells otherwise not found in the local tissue environment. The immuno-ablated strains of mice, such as nude mice, normally employed, could not represent the optimal model for this type of studies. In our reported experiments, the employment of immunocompetent recipient mice was possible because we used scaffold seeded with syngeneic MSCs.

Cells belonging to the innate immunity and, in particular, MC/Mph lead the inflammatory cascade reaction guiding revascularization and repair/regeneration of tissue at injury sites [12,13,27]. They exert this function by secreting inductive cytokines responsible for progenitor cell migration, a critical step in tissues that heal by regenerative processes rather than by a mere repair [28]. Macrophages are a heterogeneous subset of the mononuclear cell population that

comprises multiple phenotypes that are induced in response to local stimuli during the wound healing process [29]. Classically activated (M1) macrophages exhibit potent antimicrobial properties, high capacity to present antigen, and consequent activation of Th1 responses. Alternatively activated (M2) macrophages possess the capacity to facilitate tissue repair and regeneration [30].

Consistent with the MSC-mediated anti-inflammatory capacities already described by different authors [19] and with previous studies conducted using different experimental approaches [27,31], we showed that implanted MSCs caused an increased percentage of alternatively activated ($CD206^{pos}CD51^{pos}$) M2 macrophages infiltrating the ectopic implants, and a decrease in the percentage of infiltrating proinflammatory ($CD86^{pos}CD40^{pos}$) M1 macrophages. The secretory pattern of MSCs is highly influenced by their microenvironment, and, in particular, they are very sensitive to inflammatory stimuli [2,16,17]. To gain more insight in the contribution of MSCs to the tissue regeneration, we mimicked in vitro the inflammatory environment surrounding the implanted cells and we studied whether it could affect the activation of intracellular pathways and the release of factors possibly involved in the macrophage functional switch. It has been described that MSCs express high levels of IL-1Rα, enabling them to modulate the expression profile of M1 activated macrophages [32]. We here reported that, in response to the IL-1α, MSCs activated NF-kB-dependent inflammatory pathways leading to the enhanced expression of COX-2 and acute phase proteins, such as KC/CXCL1, related to angiogenesis [33], and Lcn-2, controlling the expression of the SDF-1, a chemokine playing a major role in both tissue repair and mobilization of progenitor cells [34]. We focused on COX-2 downstream enzymes since prostaglandins play an important role in modulating the macrophage cytokine profile [19]. Our in vitro data demonstrated that the MSC-mediated secretion of PGE_2 was responsible for the macrophage switch to the proresolving phenotype, and suggested that the enhanced percentage of alternatively activated macrophages in the MSC-seeded implants was related to the secretion of PGE_2. This bioactive molecule plays also a role in the control of angiogenesis and vasculogenesis, inducing the mobilization of EPCs [35].

Moreover, the polarization of macrophages skews the secretion of DAMPS, including HMGB1, as well as TNF-α, vascular endothelial growth factor (VEGF), and MMP-9 (metalloproteinase-9), all molecules involved in the regulation of cell diapedesis and migration.

In a regenerative microenvironment, both angiogenesis and vasculogenesis can occur [36]. We previously showed that the vascularization of the implant was one of the first host reactions to the graft [5,25]. To define the compartmental origin of the ECs recruited within the pores of the scaffolds, and to evaluate whether cells present in the scaffold (still present seeded MSC and host-derived macrophages) were effective at inducing BM-derived EPCs migration within the scaffold, we took advantage of the chimeric mouse model. The empty scaffold implantation induced the migration into the scaffold, of only locally resident mature $CD31^{pos}GFP^{neg}$ cells. On the contrary, seeded MSCs triggered the mobilization toward the implanted scaffold of both mature locally resident $CD31^{pos}GFP^{neg}$ cells and BM-derived $TLR2^{pos}CD133^{pos}VEGFR2^{pos}GFP^{pos}$ EPCs, indicating that the vasculature of the cell-seeded scaffolds originated from both the sprouting of pre-existing vessels and the recruitment of circulating BM progenitor cells.

In our in vivo model, donor cells were dismissed from the graft within 2–3 weeks, whereas host cells competent to form bone were recruited to a direct osteogenic function at a later time [4,5]. In principle, this phenomenon can reflect two conceivable events. Local mesenchymal cells residing in proximity of the graft site can be reprogrammed to an osteogenic fate/commitment by factors known to act as key osteogenic inducers. Alternatively, cells competent to form bone can be recruited from the circulation and/or mobilized from the BM.

Our previous published data indicated that a population of $CD146^{pos}$ cells could be recovered from the MSC-seeded scaffold, but not from the empty scaffolds, 11 days after implantation [5]. Taking advantage of the chimeric mouse model, we could determine that a significant percentage of BM derived $CD146^{pos}CD105^{pos}$ cells were recovered from the MSC-seeded scaffolds, but not from the empty scaffolds. These cells were isolated, expanded in vitro and shown to maintain an osteogenic potential after 2 months in culture. When these cells were investigated for the expression of markers characteristic of mesenchymal lineages, they were shown to express markers expressed also by pericytes. Pericytes are important in the stabilization of nascent capillaries and in the prevention of vascular regression. In fact, during angiogenesis pericytes are recruited to growing microvessels, where they directly inhibit EC proliferation and migration through contact and secretion of growth inhibitory factors [37,38]. In an osteogenic environment, pericytes can become osteoblasts and participate in the bone deposition. Taken together, our data indicate that the role of MSCs as factories of bioactive molecules could explain many of the beneficial effects observed with administration of these cells for tissue repair. The recruitment of endogenous cells toward an induced regenerative niche may represent a new strategy for tissue repair.

Acknowledgments

This work was supported partially by funds from the European Union FP7 (Project "Angioscaff" no. 214402) and from UPMC-Pittsburgh. The funders had no role in study design, data collection and analysis, decision to publish, or preparation of the manuscript.

Author Disclosure Statement

No competing financial interests exist

References

1. Caplan AI. (2005). Review: mesenchymal stem cells: cell-based reconstructive therapy in orthopedics. Tissue Eng 11:1198–1211.
2. Caplan AI and D Correa. (2011). The MSC: an injury drugstore. Cell Stem Cell 9:11–15.
3. Prockop DJ. (2009). Repair of tissues by adult stem/progenitor cells (MSCs): controversies, myths, and changing paradigms. Mol Ther 17:939–946.
4. Tasso R, A Augello, S Boccardo, S Salvi, M Caridà, F Postiglione, F Fais, M Truini, R Cancedda and G Pennesi. (2009).

Recruitment of a host's osteoprogenitor cells using exogenous mesenchymal stem cells seeded on porous ceramic. Tissue Eng Part A 15:2203–2212.
5. Tasso R, F Fais, D Reverberi, F Tortelli and R Cancedda. (2010). The recruitment of two consecutive and different waves of host stem/progenitor cells during the development of tissue-engineered bone in a murine model. Biomaterials 31:2121–2129.
6. Bianco P, PG Robey and PJ Simmons. (2008). Mesenchymal stem cells: revisiting history, concepts, and assays. Cell Stem Cell 10:313–319.
7. Sacchetti B, A Funari, S Michienzi, S Di Cesare, S Piersanti, I Saggio, F Tagliafico, S Ferrari, PG Robey, M Riminucci and P Bianco. (2007). Self-renewing osteoprogenitors in bone marrow sinusoids can organize a hematopoietic microenvironment. Cell 131:324–336.
8. Martin I, A Muraglia, G Campanile, R Cancedda and R Quarto. (1997). Fibroblast growthe factor-2 supports *ex vivo* expansion and maintenance of osteogenic precursors from human bone marrow. Endocrinology 138:4456–4462.
9. Goshima J, VM Goldberg and AI Caplan. (1991). The origin of bone formed in composite grafts of porous calcium phosphate ceramic loaded with marrow cells. Clin Orthop Relat Res 269:274–283.
10. Tasso R, M Gaetani, E Molino, A Cattaneo, M Monticone, A Bachi and R Cancedda. (2012). The role of bFGF on the ability of MSC to activate endogenous regenerative mechanisms in an ectopic bone formation model. Biomaterials 33:2086–2096.
11. Ulivi V, P Giannoni, C Gentili, R Cancedda and F Descalzi. (2008). p38/NF-kB-dependent expression of COX-2 during differentiation and inflammatory response of chondrocytes. J Cell Biochem 104:1393–1406.
12. Anghelina M, P Krishnan, L Moldovan and NI Moldovan. (2006). Monocytes/macrophages cooperate with progenitor cells during neovascularization and tissue repair: conversion of cell columns into fibrovascular bundles. Am J Pathol 168:529–541.
13. Lolmede K, L Campana, M Vezzoli, L Barsugi, R Tonlorenzi, E Clementi, ME Bianchi, G Cossu, AA Manfredi, S Brunelli and P Rovere-Querini. (2009). Inflammatory and alternatively activated human macrophages attract vessel-associated stem cells, relying on separate HMGB1- and MMP-9-dependent pathways. J Leukoc Biol 85:779–787.
14. Moldovan NI. (2002). Role of monocytes and macrophages in adult angiogenesis: a light at the tunnel's end. J Hematother Stem Cell Res 11:179–194.
15. Pusterla T, J Nemeth, I Stein, L Wiechert, D Knigin, S Marhenke, T Longerich, V Kumar, B Arnold, et al. (2013). Rage is a key regulator of oval cell activation and inflammation-associated liver carcinogenesis in mice. Hepatology 58:363–373.
16. Singer NG and AI Caplan. (2011). Mesenchymal stem cells: mechanisms of inflammation. Annu Rev Pathol 6:457–478.
17. Trento C and F Dazzi. (2010). Mesenchymal stem cells and innate tolerance: biology and clinical applications. Swiss Med Wkly 140:w13121.
18. Németh K, A Leelahavanichkul, PS Yuen, B Mayer, A Parmelee, K Doi, PG Robey, K Leelahavanichkul, BH Koller, et al. (2009). Bone marrow stromal cells attenuate sepsis via prostaglandin E(2)-dependent reprogramming of host macrophages to increase their interleukin-10 production. Nat Med 15:42–49.
19. Maggini J, G Mirkin, I Bognanni, J Holmberg, IM Piazzón, I Nepomnaschy, H Costa, C Cañones, S Raiden, M Vermeulen and JR Geffner. (2010). Mouse bone marrow-derived mesenchymal stromal cells turn activated macrophages into a regulatory-like profile. PLoS One 5:e9252.
20. Chavakis E, A Hain, M Vinci, G Carmona, ME Bianchi, P Vajkoczy, AM Zeiher, T Chavakis and S Dimmeler. (2007). High-mobility group box 1 activates integrin-dependent homing of endothelial progenitor cells. Circ Res 100:204–212.
21. Chen CW, M Corselli, B Peault and J Huard. (2012). Human blood-vessel-derived stem cells for tissue repair and regeneration. J Biomed Biotechnol 597439.
22. Kokovay E, L Li and LA Cunningham. (2006). Angiogenic recruitment of pericytes from bone marrow after stroke. J Cereb Blood Flow Metab 26:545–555.
23. Togel F, K Weiss, Y Yang, Z Hu, P Zhang and C Westenfelder. (2007). Vasculotropic, paracrine actions of infused mesenchymal stem cells are important to the recovery from acute kidney injury. Am J Physiol Renal Physiol 292:F1626–F1635.
24. Iso Y, JL Spees, C Serrano, B Bakondi, R Pochampally, YH Song, BE Sobel, P Delafontaine and DJ Prockop. (2007). Multipotent human stromal cells improve cardiac function after myocardial infarction in mice without long-term engraftment. Biochem Biophys Res Commun 354:700–706.
25. Tortelli F, R Tasso, F Loiacono and R Cancedda. (2010). The development of tissue-engineered bone of different origin through endochondral and intramembranous ossification following the implantation of mesenchymal stem cells and osteoblasts in a murine model. Biomaterials 31:242–249.
26. Caplan AI and JE Dennis. (2006). Mesenchymal stem cells as trophic mediators. J Cell Biochem 98:1076–1084.
27. Chen CP, MY Lee, JP Huang, JD Aplin, YH Wu, CS Hu, PC Chen, H Li, SM Hwang, SH Liu and YC Yang. (2008). Trafficking of multipotent mesenchymal stromal cells from maternal circulation through the placenta involves vascular endothelial growth factor receptor-1 and integrins. Stem Cells 26:550–561.
28. Schwartz M. (2010). "Tissue-repairing" blood-derived macrophages are essential for healing of the injured spinal cord: from skin-activated macrophages to infiltrating blood-derived cells? Brain Behav Immun 24:1054–1057.
29. Mantovani A, A Sica, S Sozzani, P Allavena, A Vecchi and M Locati. (2004). The chemokine system in diverse forms of macrophage activation and polarization. Trends Immunol 25:677–686.
30. Sica A and A Mantovani. (2012). Macrophage plasticity and polarization: *in vivo* veritas. J Clin Invest 122:787–795.
31. Dayan V, G Yannarelli, F Billia, P Filomeno, XH Wang, JE Davies and A Keating. (2011). Mesenchymal stromal cells mediate a switch to alternatively activated monocytes/macrophages after acute myocardial infarction. Basic Res Cardiol 106:1299–1310.
32. Ortiz LA, M Dutreil, C Fattman, AC Pandey, G Torres, K Go and DG Phinney. (2007). Interleukin 1 receptor antagonist mediates the antiinflammatory and antifibrotic effect of mesenchymal stem cells during lung injury. Proc Natl Acad Sci U S A 104:11002–11007.
33. Scapini P, M Morini, C Tecchio, S Minghelli, E Di Carlo, E Tanghetti, A Albini, C Lowell, G Berton, DM Noonan and MA Cassatella. (2004). CXCL1/macrophage inflammatory protein-2-induced angiogenesis *in vivo* is mediated by neutrophil-derived vascular endothelial growth factor-A. J Immunol 172:5034–5040.
34. Costa D, R Biticchi, S Negrini, R Tasso, R Cancedda, F Descalzi, G Pennesi and S Tavella. (2010). Lipocalin-2

controls the expression of SDF-1 and the number of responsive cells in bone. Cytokine 51:47–52.
35. Hristov M, A Zernecke, K Bidzhekov, EA Liehn, E Shagdarsuren, A Ludwig and C Weber. (2007). Importance of CXC chemokine receptor 2 in the homing of human peripheral blood endothelial progenitor cells to sites of arterial injury. Circ Res 100:590–597.
36. Madeddu P. (2005). Therapeutic angiogenesis and vasculogenesis for tissue regeneration. Exp Physiol 90:315–326.
37. Diaz-Flores L, R Gutierrez and H Varela. (1994). Angiogenesis: an update. Histol Histopathol 9:807–843.
38. Hirschi KK and PA D'Amore. (1996). Pericytes in the microvasculature. Cardiovasc Res 32:687–698.

Address correspondence to:
Prof. Ranieri Cancedda
Department of Experimental Medicine (DIMES)
University of Genova
Largo Rosanna Benzi 10
Genova 16132
Italy

E-mail: ranieri.cancedda@unige.it

Received for publication July 12, 2013
Accepted after revision August 7, 2013
Prepublished on Liebert Instant Online August 7, 2013